© 2015. Published by The Company of Biologists Ltd | Development (2015) 142, 2564-2573 doi:10.1242/dev.122648

RESEARCH ARTICLE

STEM CELLS AND REGENERATION

Stromal *Fat4* acts non-autonomously with *Dchs1/2* to restrict the nephron progenitor pool

Mazdak Bagherie-Lachidan[1,2], Antoine Reginensi[2], Qun Pan[3], Hitisha P. Zaveri[4], Daryl A. Scott[4], Benjamin J. Blencowe[1,3], Françoise Helmbacher[5] and Helen McNeill[1,2,*]

ABSTRACT

Regulation of the balance between progenitor self-renewal and differentiation is crucial to development. In the mammalian kidney, reciprocal signalling between three lineages (stromal, mesenchymal and ureteric) ensures correct nephron progenitor self-renewal and differentiation. Loss of either the atypical cadherin FAT4 or its ligand Dachsous 1 (DCHS1) results in expansion of the mesenchymal nephron progenitor pool, called the condensing mesenchyme (CM). This has been proposed to be due to misregulation of the Hippo kinase pathway transcriptional co-activator YAP. Here, we use tissue-specific deletions to prove that FAT4 acts non-autonomously in the renal stroma to control nephron progenitors. We show that loss of *Yap* from the CM in *Fat4*-null mice does not reduce the expanded CM, indicating that FAT4 regulates the CM independently of YAP. Analysis of $Six2^{-/-};Fat4^{-/-}$ double mutants demonstrates that excess progenitors in *Fat4* mutants are dependent on *Six2*, a crucial regulator of nephron progenitor self-renewal. Electron microscopy reveals that cell organisation is disrupted in *Fat4* mutants. Gene expression analysis demonstrates that the expression of Notch and FGF pathway components are altered in *Fat4* mutants. Finally, we show that *Dchs1*, and its paralogue *Dchs2*, function in a partially redundant fashion to regulate the number of nephron progenitors. Our data support a model in which FAT4 in the stroma binds to DCHS1/2 in the mouse CM to restrict progenitor self-renewal.

KEY WORDS: *Fat4*, *Dachsous 1*, Progenitor renewal, Stroma, Hippo pathway

INTRODUCTION

Determining how organ size is regulated, and how progenitor cells self-renew, is crucial for understanding normal development. The mammalian kidney derives from three interdependent lineages: the ureteric bud (UB), which forms the collecting ducts; the nephron progenitors, also known as condensing or cap mesenchyme (CM), which both self-renew and undergo a mesenchymal-to-epithelial transition (MET) to give rise to the nephron; and the loosely associated mesenchymal-like cells known as the stroma.

Stromal cells regulate both UB renal branching and the balance between self-renewal and nephron differentiation of the CM (Batourina et al., 2001; Das et al., 2013; Hatini et al., 1996; Hum et al., 2014; Levinson et al., 2005; Mendelsohn et al., 1999, 1994; Paroly et al., 2013). Loss of the stromal transcription factor gene *Foxd1* results in reduced branching and an expanded CM (Hatini et al., 1996). Similarly, loss of the stromal transcription factor genes *Pbx1* (Schnabel et al., 2003), *Pod1* (*Tcf21* – Mouse Genome Informatics) (Quaggin et al., 1999) or the atypical cadherin gene *Fat4* (Das et al., 2013; Saburi et al., 2008) also results in an excessive CM. How these stromally expressed genes regulate self-renewal and/or differentiation of the CM remains to be determined.

The *Drosophila* tumour suppressor Fat (Ft) is a large atypical cadherin that regulates cell adhesion (Fanto et al., 2003; Matakatsu and Blair, 2006), planar cell polarity (PCP) (Fanto et al., 2003; Rawls et al., 2002; Yang et al., 2002), growth (Bennett and Harvey, 2006; Bryant et al., 1988; Silva et al., 2006; Willecke et al., 2006) and metabolism (Sing et al., 2014). The vertebrate family of FAT cadherins is composed of four cadherins (FAT1-4). FAT4 is considered to be the orthologue of Ft based on homology of the intracellular domain and the ability of the FAT4 cytoplasmic domain to rescue PCP defects of *Drosophila ft* mutants (Pan et al., 2013). $Fat4^{-/-}$ mice fail to establish proper PCP in the kidney tubules, resulting in the formation of renal cysts (Saburi et al., 2008). *Fat1* is required for renal slit junction formation (Ciani et al., 2003), and synergises with *Fat4* in cyst repression (Saburi et al., 2012). *Fat2* is the only FAT family cadherin not expressed in the developing kidney (Barlow et al., 2010; Rock et al., 2005). *Fat3* is expressed in the developing kidney (Rock et al., 2005), and acts synergistically with *Fat4* to regulate cyst development (Saburi et al., 2012).

Dachsous (Ds) is a large atypical cadherin that binds *Drosophila* Ft, and regulates growth, adhesion and PCP [reviewed by Sharma and McNeill (2013)]. Dachsous 1 (DCHS1) and Dachsous 2 (DCHS2) are the two mammalian orthologues of *Drosophila* Ds. Mao et al. (2011) showed that *Dchs1* mutants have similar phenotypes to *Fat4* mutants, including cystic kidneys. *Dchs2* is also expressed in the kidney, but no genetic study has yet addressed the function of *Dchs2*.

Fat4 mutants have an expanded CM population surrounding the UB tips (Das et al., 2013; Mao et al., 2011; Saburi et al., 2008). *Drosophila* Ft regulates the Hippo kinase pathway, a conserved growth-controlling pathway that regulates the transcriptional co-activator protein Yorkie via inhibitory phosphorylations. The mammalian homologues of Yorkie are called YAP and TAZ. Recently, Das et al. (2013) reported that YAP levels were increased and phosphorylated-YAP (pYAP) was decreased in the CM of *Fat4* mutants. They proposed that FAT4 regulates the progenitor pool by increasing nuclear YAP in the CM non-autonomously, possibly by binding to FAT3 or DCHS1 in the CM.

Here, we use tissue-specific analyses with Cre recombinase in mice to demonstrate that *Fat4* regulates the CM non-autonomously by acting in the stroma. We show that CM formation is not affected by

[1]Department of Molecular Genetics, University of Toronto, Toronto, Ontario, Canada M5S 1A8. [2]Lunenfeld-Tanenbaum Research Institute, Mt. Sinai Hospital, Toronto, Ontario, Canada M5G 1X5. [3]Terrence Donnelly Centre for Cellular and Biomolecular Research, University of Toronto, Toronto, Ontario, Canada M5S 3E1. [4]Department of Molecular and Human Genetics, Baylor College of Medicine, Houston, TX 77030, USA. [5]Institut du Développement de Marseille, CNRS UMR 7288, France.

*Author for correspondence (mcneill@lunenfeld.ca)

Received 28 January 2015; Accepted 18 June 2015

Development (2015) 142, 2564-2573 doi:10.1242/dev.122648

the core PCP pathway, and that *Dchs1* and *Dchs2* act in a partially redundant fashion to control mesenchymal progenitor cell number. We further show that *Fat1* and *Fat3* are not required to regulate nephron progenitors, and that loss of *Yap* in the CM does not reduce the excess progenitors found in *Fat4* mutants. Electron microscopy (EM) analysis reveals that *Fat4* mutants have defective cellular organisation in both the CM and the UB-derived epithelial tubules. mRNA expression analysis of *Fat4* mutants reveals alterations in Notch and FGF pathway components. Taken together, our data indicate that FAT4 in the stroma binds to DCHS1 and DCHS2 in the CM to regulate nephron progenitors, independently of YAP in the CM, and that loss of *Fat4* disrupts multiple signalling pathways.

RESULTS

Loss of *Fat4* results in expansion of the condensing mesenchyme

Loss of *Fat4* results in an expanded CM that is visible in histological sections (Fig. 1A,B). To understand better how loss of *Fat4* leads to excess CM, we carefully characterised *Fat4*$^{-/-}$ kidney development, using antibodies against SIX2 to label the CM and cadherin 1 (ECAD) to label the UB. This analysis showed that loss of *Fat4* results in an expanded CM population that is obvious from embryonic day (E) 12.5 to birth (Fig. 1G-L; supplementary material Fig. S1A-F). Quantification of the CM progenitor pool surrounding each UB confirms an almost twofold increase in the number of nephron progenitors (e.g. at E13.5 there was an average of 95 cells/UB in wild type versus 181 cells/UB in *Fat4*$^{-/-}$ mutants; Fig. 1M). Staining with other CM markers, such as CITED1, PAX2 and SALL1, confirm expansion of the CM, and the presence of the stromal markers PBX1, FOXD1 and tenascin C (TEN; TNC – Mouse Genome Informatics) (Fig. 1G-L; Fig. 4E-J) demonstrate an apparently normal-sized stroma. Quantification of glomeruli number showed reduced nephrogenesis at postnatal day (P) 0 in *Fat4* mutants, suggesting a delay in epithelialisation (supplementary material Fig. S1M-O).

Electron microscopy reveals early loss of cell organisation in *Fat4* mutants

To obtain a better insight into the cellular mechanism underlying the increased CM observed in *Fat4* mutants, we used ultrathin sections and EM to examine *Fat4* mutants. In controls at E12.5, the normal tight organisation of mesenchymal cells surrounding an inducing UB tip was easily observed (Fig. 1C). EM analysis of *Fat4*$^{-/-}$ kidneys at E12.5 showed a larger CM surrounding the epithelial tubules (Fig. 1D). In addition, both the epithelial tubules and the CM of *Fat4* nulls were distorted and showed a lack of tight organisation (Fig. 1C-F). This lack of tissue organisation could reduce the efficacy of signalling from the UB tip to the CM.

Fat1 and *Fat3* do not restrict CM size

It has been speculated that *Fat4* might act through other FAT cadherins, such as FAT3, to regulate the CM progenitor pool

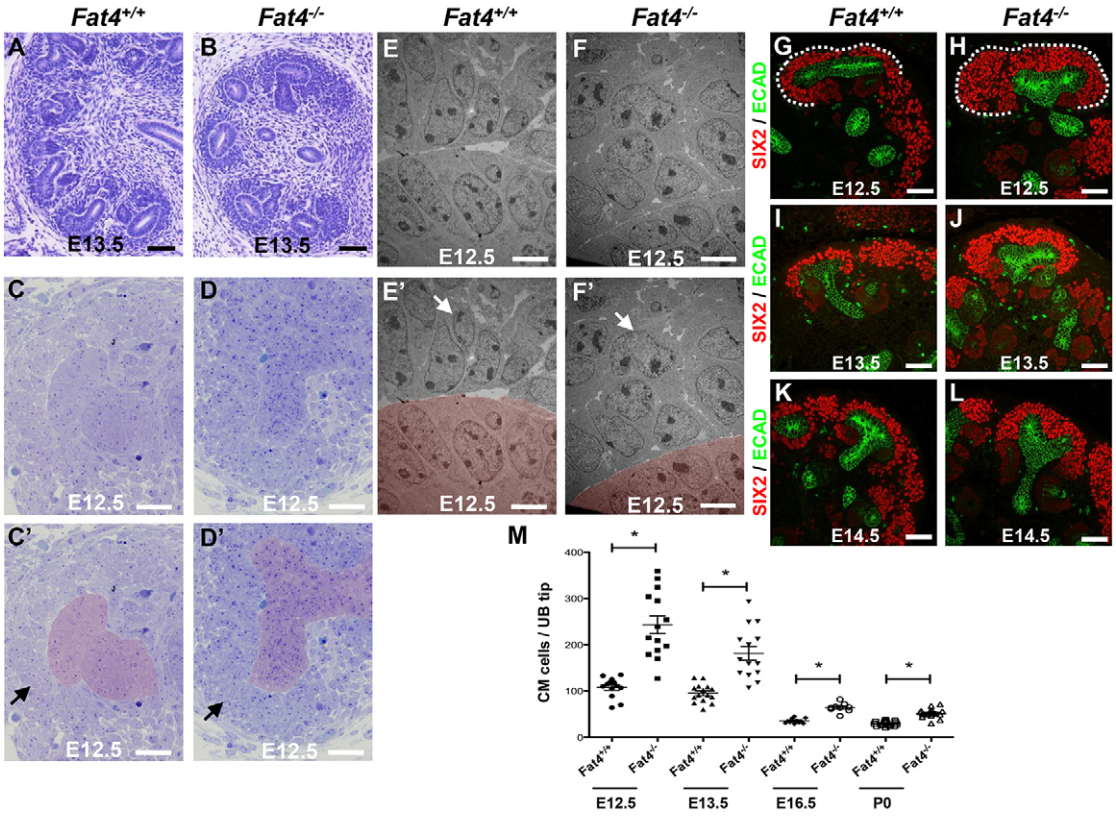

Fig. 1. Loss of *Fat4* results in expansion of the renal progenitor pool. (A,B) Histological analyses (PAS) of E13.5 embryonic mouse kidneys show an expanded condensing mesenchyme (CM) in *Fat4*$^{-/-}$ mutants. (C-D′) Electron microscopy of E12.5 kidneys reveal that both the epithelial (pseudocoloured in light red in C′,D′) and surrounding CM (marked by arrows) compartments are disorganised at the tissue level. (E-F′) Upon closer examination, CM cells (top half and marked by an arrow in E′,F′) appear to have more extracellular matrix and are more disorganised in *Fat4* mutants. The ureteric bud (UB) compartment is pseudocoloured in E′ and F′. (G-L) IF staining with SIX2 (CM) and ECAD (UB) antibodies shows the expansion of the CM in *Fat4*$^{-/-}$ embryos from E12.5 to E14.5. Dotted lines outline the CM. (M) Quantification of the number of CM cells per UB demonstrate that *Fat4* mutants have an expanded CM from E12.5 until birth. **P*<0.0001. Scale bars: 50 µm in A,B,G-L; 100 µm in C-D′; 6 µm in E-F′.

Development (2015) 142, 2564-2573 doi:10.1242/dev.122648

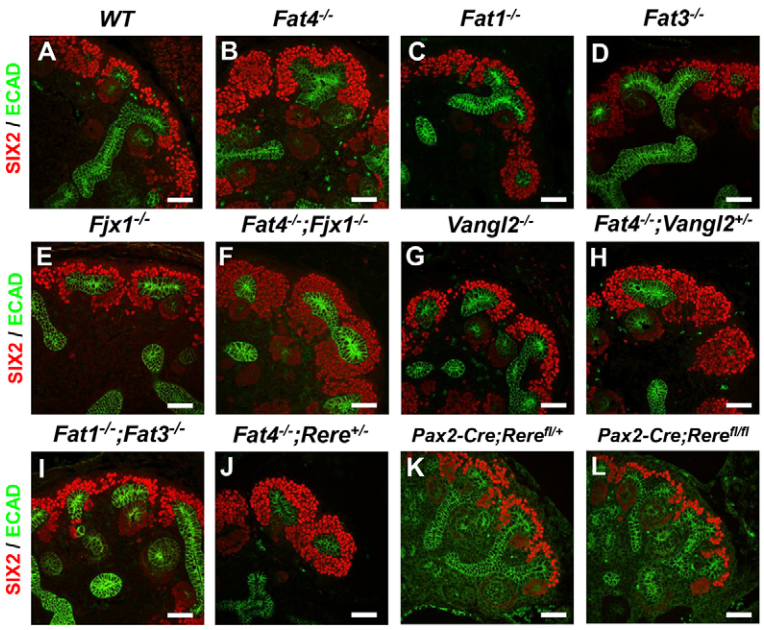

Fig. 2. *Fat4* maintains the renal progenitor pool independently of other FAT cadherins, *Fjx1*, *Rere* and *Vangl2*. (A-L) *Fat1*$^{-/-}$ and *Fat3*$^{-/-}$ kidney have a normal CM population (C,D versus A). *Fat1*$^{-/-}$;*Fat3*$^{-/-}$ double mutants also have a normal CM (I versus A). Loss of *Four-jointed box 1* (*Fjx1*) does not result in an expanded CM (E), and *Fat4*$^{-/-}$;*Fjx1*$^{-/-}$ double mutants (F) phenocopy *Fat4*$^{-/-}$ single mutants, suggesting that *Fjx1* does not have a role in determining the renal progenitors. *Vangl2* single mutants have a normal CM population (G versus A), whereas *Fat4*$^{-/-}$;*Vangl2*$^{+/-}$ double mutants have a renal progenitor pool that resembles *Fat4*$^{-/-}$single mutants (H versus B). *Fat4*$^{-/-}$;*Rere*$^{+/-}$ double mutants phenocopy *Fat4*$^{-/-}$ single mutants (J versus B). Mutants in which *Rere* is absent specifically from the CM and UB compartments also have a regular CM (K,L). Embryos shown are at E13.5, except for K,L, which are at E15.5. Antibodies against SIX2 (CM) and ECAD (UB) were used. Scale bars: 50 µm.

(Das et al., 2013). *Fat1*, *Fat3* and *Fat4* are the only FAT cadherins expressed during kidney development (Rock et al., 2005). We therefore examined the CM of *Fat1*$^{-/-}$ and *Fat3*$^{-/-}$ single mutants by staining embryonic kidneys with antibodies to SIX2 and ECAD (Fig. 2A-D). This revealed a normal CM in both *Fat3*$^{-/-}$ and *Fat1*$^{-/-}$ single mutants. We also found that *Fat1*$^{-/-}$;*Fat3*$^{-/-}$ double mutants had a normal-sized CM (Fig. 2I). Thus, *Fat4* has a unique role in regulating the CM, and does not act through *Fat1* or *Fat3* to control the nephron progenitor pool.

Loss of *Dchs1* results in an expansion of the condensing mesenchyme

Drosophila dachsous (*ds*) has two mammalian orthologues (*Dchs1* and *Dchs2*). Previous work has shown that loss of *Dchs1* results in renal cysts, albeit to a lesser extent than that observed in *Fat4* mutants (Mao et al., 2011). We examined *Dchs1*$^{-/-}$ mutants and found that loss of *Dchs1* phenocopies the expanded *Fat4* CM (Fig. 3A,B). Staining with several CM markers confirmed excess progenitors in *Dchs1* mutants (Fig. 3E-J). Quantification of the CM population surrounding each UB confirmed expansion of the CM in *Dchs1*$^{-/-}$ kidneys (average 115 cells/UB in wild type versus average 171 cells/UB in *Dchs1*$^{-/-}$) (Fig. 3K). *Dchs1*$^{-/-}$ mutants had a slightly smaller CM population compared with *Fat4*$^{-/-}$ mutants (average 171 cells/UB versus 181 cells/UB); however, this was not statistically significant. Immunofluorescence (IF) and *in situ* hybridisation (ISH) analyses of *Dchs1* revealed highest expression in the stroma and mesenchyme, with weak expression in the UB (supplementary material Fig. S2B,C,G,H). Interestingly, DCHS1 expression is increased in *Fat4* mutants (supplementary material Fig. S2I,J; Mao et al., 2011).

Dchs2 is partially redundant with *Dchs1* in regulation of the progenitor pool

We wondered whether the *Dchs1* paralogue *Dchs2* might also play a role in the regulation of nephron progenitors. *Dchs2* is expressed at low levels throughout the developing kidney (supplementary material Fig. S2). We generated *Dchs2*-null mice, and determined that they were viable and fertile (F.H., unpublished). Analysis of *Dchs2* mutants showed a normal-sized CM (Fig. 3C,K). To determine whether there is a synergistic relationship between *Dchs1* and *Dchs2*, we generated and examined *Dchs1*$^{-/-}$;*Dchs2*$^{-/-}$ double mutants and stained for SIX2 and ECAD (Fig. 3D). Importantly, quantification revealed that *Dchs1*$^{-/-}$;*Dchs2*$^{-/-}$ mutants have an expanded CM population that is larger than that of *Dchs1* single mutants (Fig. 3D,K). Thus, *Dchs1* and *Dchs2* are partially redundant in the regulation of the progenitor pool.

The PCP genes *Vangl2*, *Atn1*, *Rere* and *Fjx1* do not affect CM size

Drosophila Ft and Ds regulate PCP in the wing and eye [reviewed by Sharma and McNeill (2013)]. Atrophin (Grunge – FlyBase) is a nuclear co-repressor that functions with Ft to regulate PCP in the *Drosophila* eye (Fanto and McNeill, 2004). Two mammalian orthologues of *Atrophin* exist in mammals: *atrophin 1* (*Atn1*) and *atrophin 2* (*Rere*). *Atn1* mutants are viable and fertile, with a normal CM (data not shown). *Rere*$^{-/-}$ mutants die at ∼E9.5 (Zoltewicz et al., 2004). We find that *Rere*$^{+/-}$ single mutants had a normal CM (supplementary material Fig. S3B,C) and *Fat4*$^{-/-}$;*Rere*$^{+/-}$ double mutants have an expanded CM that is similar to that of *Fat4* single mutants (Fig. 2J). To assess more directly RERE function in the CM, we generated *Rere*$^{flox/flox}$ conditional null mutants (D.A.S., unpublished). Removal of *Rere* with *Pax2-Cre* did not affect the size of the CM (Fig. 2K,L). Thus, alterations in *Atn1* and *Rere* do not disrupt CM self-renewal and/or differentiation.

Vangl2 is an essential component of the core PCP pathway (Simons and Mlodzik, 2008). Loss of *Vangl2* results in a reduced number of glomeruli and reduced branching (Babayeva et al., 2011; Yates et al., 2010). Staining with a SIX2 antibody revealed that *Vangl2*$^{-/-}$ single mutants have a normal CM, and that *Fat4*$^{-/-}$;*Vangl2*$^{+/-}$ double mutants have a CM population similar in size to that of *Fat4* single mutants (Fig. 2G,H).

Drosophila Four-jointed (Fj), is a Golgi-localised kinase that has roles in both PCP and Hippo growth regulation [reviewed by Sharma and McNeill (2013)]. *fj* has a single mammalian orthologue, *Fjx1*, which has increased expression in both *Drosophila fat* and mouse *Fat4*$^{-/-}$ mutants (supplementary material Fig. S1P,Q; Saburi et al., 2008). Staining of *Fjx1*$^{-/-}$ kidneys with a SIX2 antibody showed a normal CM, suggesting that *Fjx1* is not essential for

Development (2015) 142, 2564-2573 doi:10.1242/dev.122648

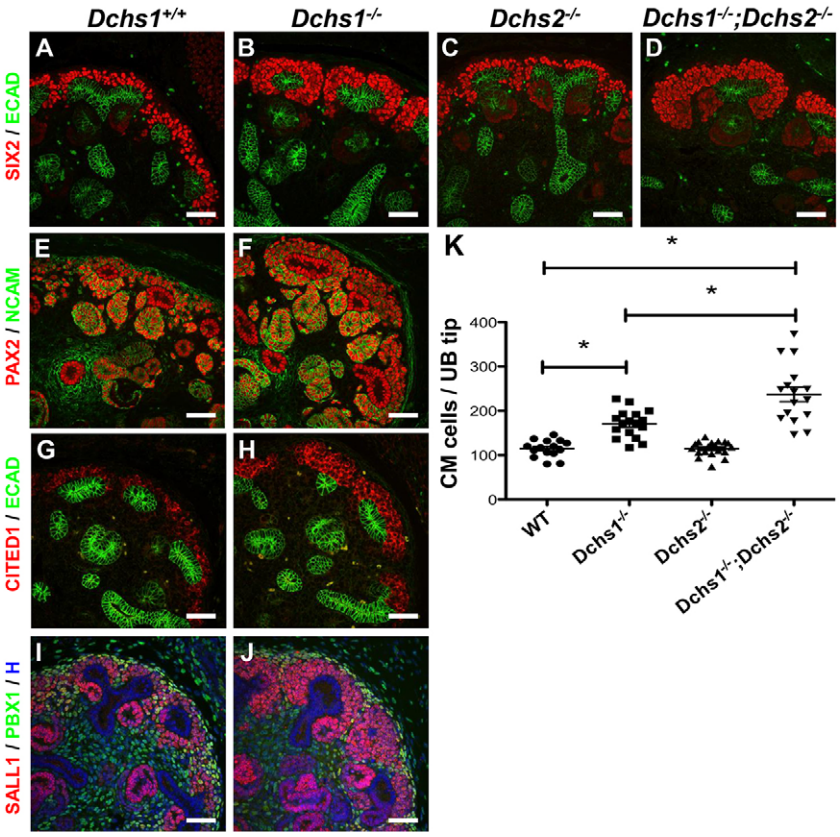

Fig. 3. *Dchs1/2* maintain the renal progenitor pool. (A-K) Loss of dachsous 1 (*Dchs1*) results in an expansion of the CM similar to that observed in *Fat4* mutants (A,B; all embryos shown and quantified in this figure are at E13.5). Staining with PAX2, CITED1 and SALL1 antibodies confirms that the CM is expanded in *Dchs1* mutants (E-J). Although *Dchs2* single mutants (C) have a normal CM population, $Dchs1^{-/-};Dchs2^{-/-}$ double mutants (D) have a larger CM than *Dchs1* single mutants. (K) Quantification of the number of CM cells surrounding each UB confirms our findings.*$P<0.0001$. H, Hoechst. Scale bars: 50 µm.

regulating the size of the progenitor pool (Fig. 2E). To determine whether increased *Fjx1* expression in *Fat4* mutants is responsible for the enhanced CM of *Fat4* mutants, we examined $Fat4^{-/-};Fjx1^{-/-}$ double mutants. $Fat4^{-/-};Fjx1^{-/-}$ double mutants phenocopy *Fat4* single mutants (Fig. 2F), indicating that increased FJX1 is not responsible for the increased CM size of *Fat4* mutants. Taken together, our results indicate that *Atn1*, *Rere*, *Vangl2* and *Fjx1* are not required for nephron progenitor regulation.

Fat4 is expressed throughout the kidney, with strongest expression in the stroma

To understand better how *Fat4* and *Dchs1* regulate progenitors, we examined their expression patterns. Using both ISH and a $Fat4^{EGFP/+}$ knock-in reporter line (Wu et al., 2008), we found that *Fat4* has highest expression in the stroma, moderate expression in the CM and weak expression in the UB (Fig. 4A-D). The stromal compartment of *Fat4* mutants still expresses the stromal markers FOXD1 and PBX1, along with increased tenascin C expression in the stroma (Fig. 4E-H).

Fat4 acts in the cortical stroma to regulate renal progenitors

To determine where *Fat4* acts to control progenitor pool size, *Fat4* was removed from different lineages. Removal of *Fat4* from the UB (*Hoxb7-Cre;*$Fat4^{flox/-}$) or the CM (*Six2-Cre;*$Fat4^{flox/-}$) lineages did not result in an expanded CM population (Fig. 5D,E). Thus, *Fat4* does not act in the epithelium or in the CM to regulate MET. However, by contrast, we found that removal of *Fat4* only from the stroma ($Foxd1^{Cre/+};Fat4^{flox/-}$) resulted in an expanded CM population, similar in size to that of *Fat4* mutants (Fig. 5F). Therefore, *Fat4* in the stroma non-autonomously regulates the size of the CM.

The stromal compartment can be subdivided into three layers: (1) the capsular stroma (single layer of cells surrounding the developing kidney proper); (2) the cortical stroma (peripherally localised cells that surround the UB and the CM); and (3) the medullary stroma (the inner kidney) (Cullen-McEwen et al., 2005; Li et al., 2014). $Foxd1^{Cre/+}$ excises from both cortical and medullary stromal compartments (Humphreys et al., 2010; Kobayashi et al., 2014). *Pax3* is expressed throughout the kidney, with mosaic expression in both the UB and the CM, and is strongly expressed in the medullary and cortical stroma (Engleka et al., 2005). We found that $Pax3^{Cre/+};Fat4^{flox/-}$ kidneys also exhibited large CM condensates similar to those observed in *Fat4* nulls and $Foxd1^{Cre/+};Fat4^{flox/-}$ conditional mutants (Fig. 5C). To determine whether *Fat4* is acting in the cortical or medullary stroma, we examined *Rarb2-Cre;*$Fat4^{flox/-}$ kidneys because *Rarb2-Cre* excises from the CM and medullary stroma but not from the cortical stroma (Di Giovanni et al., 2011; Kobayashi et al., 2005). Interestingly, *Rarb2-Cre;*$Fat4^{flox/-}$ kidneys (supplementary material Fig. S3D,E) have a normal-sized CM. Taken together, our results indicate that *Fat4* acts non-autonomously in the cortical stroma to regulate the renal progenitor pool.

Fat4 regulates the CM independently of control of YAP function in the CM

Previous studies stated that loss of *Fat4* in E15.5 embryos result in increased *Yap* expression in the CM and decreased pYAP, and proposed that increased nuclear YAP in the CM regulates nephron progenitor pool size (Das et al., 2013). To explore this potential link, we stained for YAP and phosphorylated-YAP (pYAP) in *Fat4* null and $Foxd1^{Cre/+};Fat4^{flox/-}$ mutants. We were unable to detect any differences in YAP or pYAP in *Fat4* null or $Foxd1^{Cre/+};Fat4^{flox/-}$ conditional mutants by IF at E13.5, E14.5 and P0 (supplementary material Fig. S4; data not shown). Western blots of *Fat4* mutants and controls also did not reveal consistent differences in pYAP expression levels (supplementary material Fig. S4).

Development (2015) 142, 2564-2573 doi:10.1242/dev.122648

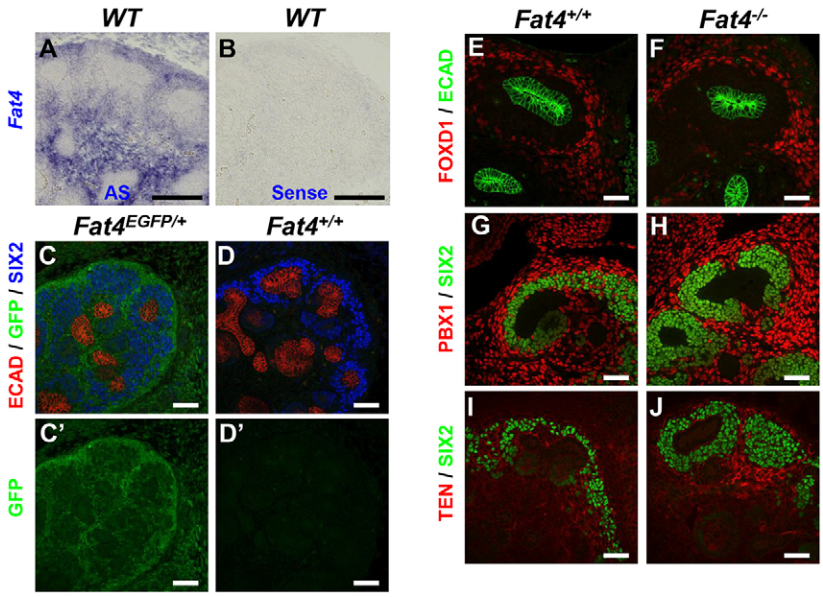

Fig. 4. *Fat4* is expressed primarily in the stromal and mesenchymal compartments of the kidney. (A-D′) ISH analysis and a $Fat4^{EGFP/+}$ knock-in reporter mouse line show that *Fat4* is expressed strongly in the stroma, moderately in the CM and faintly in the epithelial compartment. The expression pattern of the *Fat4* antisense (AS) riboprobe is shown in A, whereas B is a sense control of E13.5 kidneys. IF using a GFP antibody confirms the expression pattern of *Fat4* in a E13.5 $Fat4^{EGFP/+}$ kidney (C), whereas a no-GFP control $Fat4^{+/+}$ does not express GFP (D). C′ and D′ show the GFP channel only. (E-J) Loss of *Fat4* does not result in a loss of the stromal population in the kidney, as $Fat4^{-/-}$ mutants express the stromal markers FOXD1 (E,F) and PBX1 (G,H), whereas tenascin C (TEN) is increased in *Fat4* single mutants (I,J). Scale bars: 100 µm in A,B; 50 µm in C-J.

It is possible that subtle changes in YAP levels or phosphorylation were not detectable with our approaches. We reasoned that if loss of *Fat4* indeed functions by increasing nuclear YAP, then removal of *Yap* in the CM of a *Fat4* mutant should rescue the expanded CM phenotype. We examined $Fat4^{-/-};Yap^{+/-}$ double mutants, and found that they phenocopy *Fat4* single mutants in CM size (Fig. 6A-C), suggesting that changes in YAP levels in the CM are not the crucial mediators of excess CM in *Fat4* mutants.

$Yap^{-/-}$ mutants die at ~E9.5, so to test directly whether increased YAP mediates the increased progenitors in *Fat4* null mutants, we used conditional alleles to remove *Yap* solely from the CM in *Fat4* mutants (i.e. a $Fat4^{-/-};Six2\text{-}Cre;Yap^{flox/flox}$ mutant) (Fig. 6D-I). We found that *Yap* is efficiently excised from the CM (supplementary material Fig. S4). Significantly, these mutants phenocopied *Fat4* single mutants (i.e. there was no rescue of the expanded CM phenotype), demonstrating that the increased CM in *Fat4* mutants is not due to excess nuclear YAP in the CM.

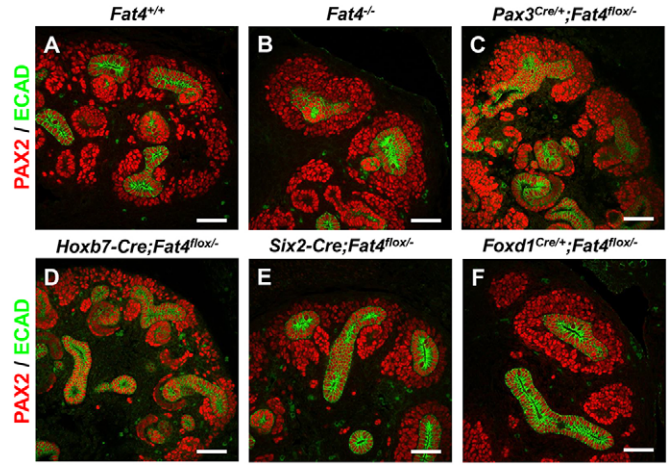

Fig. 5. *Fat4* acts non-autonomously in the stroma to regulate renal progenitors. (A-F) Removal of *Fat4* from either the UB compartment using a *Hoxb7-Cre* (D) or from the CM using a *Six2-Cre* (E) result in a normal CM population identical to that of wild type (A). Removal of *Fat4* from the stromal, CM and UB compartments using a $Pax3^{Cre/+}$ (C) phenocopies *Fat4* nulls (B). Removal of *Fat4* solely from the stromal compartment (F) results in an expanded CM similar to that of $Fat4^{-/-}$ mutants (B). Kidneys were examined at E13.5 using IF and stained with antibodies against PAX2 (CM+UB) and ECAD (UB). Scale bars: 50 µm.

Notch and FGF pathway genes are altered in *Fat4* mutants

To obtain an unbiased global view of changes in gene expression in *Fat4* mutants, we isolated kidneys from $Fat4^{-/-}$ mutants and $Fat4^{+/+}$ controls at E13.5, and conducted RNA sequencing of the transcriptome. Consistent with the increased CM of *Fat4* mutants seen in histological and marker analysis, $Fat4^{-/-}$ kidneys have increased expression of progenitor genes, including *Six2*, *Sall1*, *Gas1*, *Meox2* and *Eya1* (Fig. 7A). There is a moderate reduction of some stromal genes (*Pod1*, *Pbx1*; Fig. 7A). No change in expression was detected in the YAP target gene *Ctgf* or the canonical Wnt pathway target *Axin2* (Fig. 7C). Interestingly, global analysis of gene expression showed significant changes in several components of the Notch and FGF pathways (Fig. 7B,C). These data confirm that loss of *Fat4* leads to increased expression of progenitor markers, and show that multiple pathways known to regulate the CM (Boyle et al., 2011; Di Giovanni et al., 2015) are disrupted in *Fat4* mutants.

Six2 is necessary for the increased progenitor pool of *Fat4* mutants

Our staining and transcriptome analyses indicate that loss of *Fat4* results in increased expression of *Six2* and expansion of $SIX2^+$ cells. Previous studies have shown that *Six2* is a crucial regulator of the progenitor pool (Kobayashi et al., 2008; Self et al., 2006), suggesting that the increase in *Six2* expression might be important for the increased CM of *Fat4* mutants. We therefore examined $Six2^{-/-};Fat4^{-/-}$ mutants. Strikingly, $Six2^{-/-};Fat4^{-/-}$ mutants have a depleted progenitor pool, with precocious epithelialisation similar to that observed in $Six2^{-/-}$ mutants (Fig. 7D). These data indicate that *Six2* is epistatic to *Fat4*, and suggest that *Six2* acts downstream of, or in parallel to, *Fat4* to regulate the progenitor pool.

DISCUSSION

We have shown here that *Fat4* functions non-autonomously to regulate the size of the nephron progenitor pool. We further show that *Fat4* is the only FAT cadherin the loss of which results in an expanded CM and find similar phenotypes in $Dchs1^{-/-}$ mutants.

Development (2015) 142, 2564-2573 doi:10.1242/dev.122648

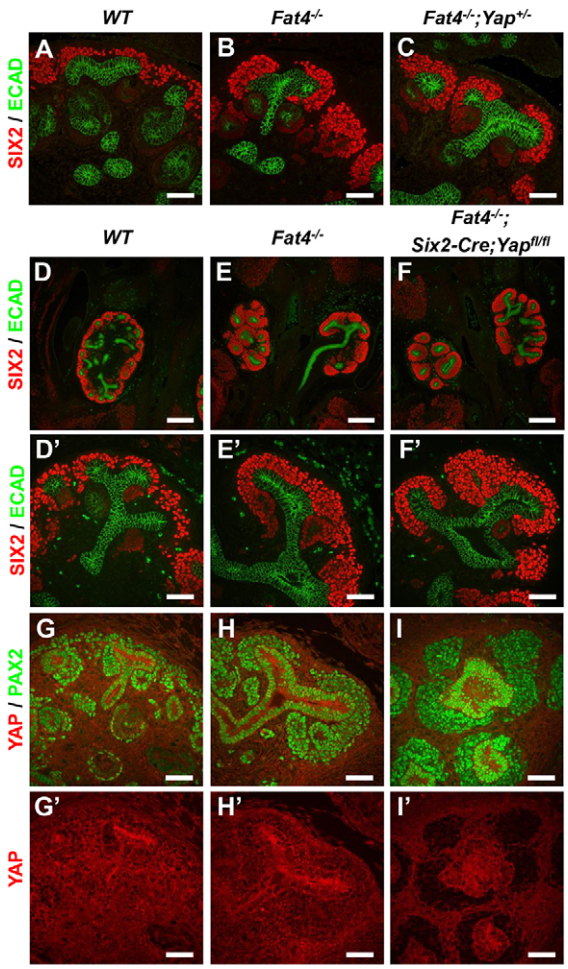

Fig. 6. *Fat4* regulates the renal progenitor pool independently of YAP. (A-I′) *Fat4*$^{-/-}$ mutants (B) are identical to *Fat4*$^{-/-}$;*Yap*$^{+/-}$ double mutants (C) as both mutants have expanded CMs compared with control wild-type kidneys (A). E13.5 kidneys were examined with antibodies against SIX2 (CM marker) and ECAD (UB marker) to examine the two populations. Removal of both *Yap* alleles from the CM compartment (using a *Six2-Cre*) in a *Fat4* null background (F,F′) phenocopies *Fat4*$^{-/-}$ single mutants (E,E′), which have an expanded CM compared with controls (D,D′). I and I′ confirm loss of YAP from the CM population compared with *Fat4*$^{-/-}$ (H,H′) and wild-type controls (G,G′). Scale bars: 200 µm in D-F; 50 µm A-C,D′-F′,G-I′.

Importantly, we also find there is a strongly expanded CM in *Dchs1*$^{-/-}$;*Dchs2*$^{-/-}$ double mutants. These data suggest that FAT4 in the stroma binds to DCHS1 and DCHS2 to non-autonomously restrict the number of CM progenitors. How and where does this signalling occur? In *Drosophila*, when Ft and Ds bind, there is evidence for signalling occurring in both directions (reviewed by Sharma and McNeill, 2013), with some of this signalling mediated by the Ft and Ds intracellular domains. As there is clear conservation not only between the cytoplasmic domains of Fat and FAT4, but also between Ds and DCHS1 and DCHS2, this raises the possibility of bidirectional signalling during regulation of the nephron progenitor pool. A signal could be generated via Dachsous cytoplasmic signalling in the nephron progenitors or downstream of FAT4 in the stromal cells, leading to restriction of the progenitor pool.

Dchs1 regulates CM size cell-autonomously (Mao et al., 2015), and, as we have shown here, *Fat4* is needed in the stromal population to regulate CM size. Therefore, the interface between the CM and the stroma is a likely place for a FAT4-DCHS1/2 signal to occur. The CM is normally two to three cell layers thick. How the FAT4-DCHS1/2 signal passes through this cell layer is not clear. Cell motility could result in different cells being involved in a FAT4-DCHS1/2 contact over time, or alternatively a diffusible signal could be generated as a result of a FAT4-DCHS1/2 interaction. Further detailed molecular and cellular studies will be needed to ascertain how FAT4 and DCHS1 signal at this interface.

Drosophila Ft and Ds binding regulates PCP. To determine whether mammalian PCP affects nephron progenitors, we examined *Fjx1*, *Atn1*, *Rere* and *Vangl2* mutants. Loss of these genes, or loss of one of these genes in a *Fat4*-null background did not affect the renal progenitor pool. Together, these data suggest that *Fat4* regulation of progenitors is not via the core PCP pathway or via the atrophin-PCP pathway.

Fat4 is expressed predominantly in the stroma, with moderate expression in the mesenchyme and weak expression in the UB. Removal of *Fat4* from the stromal population using *Foxd1*$^{Cre/+}$ resulted in excess nephron progenitors, demonstrating that *Fat4* acts non-autonomously to control the CM. *Foxd1* is expressed in both cortical and medullary interstitial stromal cells (Kobayashi et al., 2014). When *Fat4* was excised only from the medullary stroma using *Rarb2-Cre*, the CM appeared to be normal. These results suggest that *Fat4* acts from the cortical stromal layer to regulate nephron progenitors.

Recently, a stromaless kidney (produced by expression of diphtheria toxin in the *Foxd1* lineage) was shown to phenocopy *Fat4* nulls (Das et al., 2013; Hum et al., 2014). Owing to complete removal of the stromal compartment, the authors were unable to determine if a single molecular factor was responsible for the increased CM observed. We note that the increase of CM pool size in the stromaless kidney is greater than that observed in the *Fat4* mutant (Das et al., 2013), which may be due to other factors, or due to secondary proliferation subsequent to death/injury caused by the diphtheria toxin. We note that dying cells are known to release signals that promote proliferation of adjacent cells (Chera et al., 2009; Huang et al., 2011; Smith-Bolton et al., 2009), and that Yki/YAP levels increase after tissue damage, and are essential for repair and regeneration. Our genetic data clearly show that *Fat4* is a crucial stromal regulator of the CM. As we see only subtle decreases in *Foxd1*, *Pbx1* and *Pod1*, the effect of *Fat4* is unlikely to be mediated by regulation of the expression of these genes.

Our studies indicate that *Fat4* acts non-autonomously in the stroma, and suggests a model in which FAT4 signals to DCHS1 in the CM. We find that YAP and pYAP levels do not change in *Fat4* mutants during renal development (E11.5-P0), suggesting that YAP is not essential for the excess CM seen in *Fat4* mutants. We cannot account for the difference in staining between our analysis and that of Das and co-workers (Das et al., 2013); however, we note that they only reported changes in YAP expression at E15.5, days after the excessive CM becomes obvious. We note that YAP levels are slightly lower in the CM of wild-type animals, and as the CM is expanded in *Fat4* mutants, this could give an impression of lower YAP in *Fat4* nulls.

Our genetic analyses clearly demonstrate that *Fat4* does not control nephron progenitors solely through regulation of YAP in the CM, as removal of *Yap* from the SIX2^{+} renal population does not rescue the excess CM observed in *Fat4* nulls. It is possible that the YAP paralogue TAZ could play a role; however, *Fat4*$^{-/-}$;*Taz*$^{-/-}$ kidneys have an expanded CM (Mao et al., 2015), indicating that TAZ is also not essential for the increased CM of *Fat4* mutants. As we have yet to examine *Fat4*$^{-/-}$;*Six2-Cre*;*Yap*$^{flox/flox}$;*Taz*$^{flox/flox}$ mutants, we cannot exclude the possibility

Development (2015) 142, 2564-2573 doi:10.1242/dev.122648

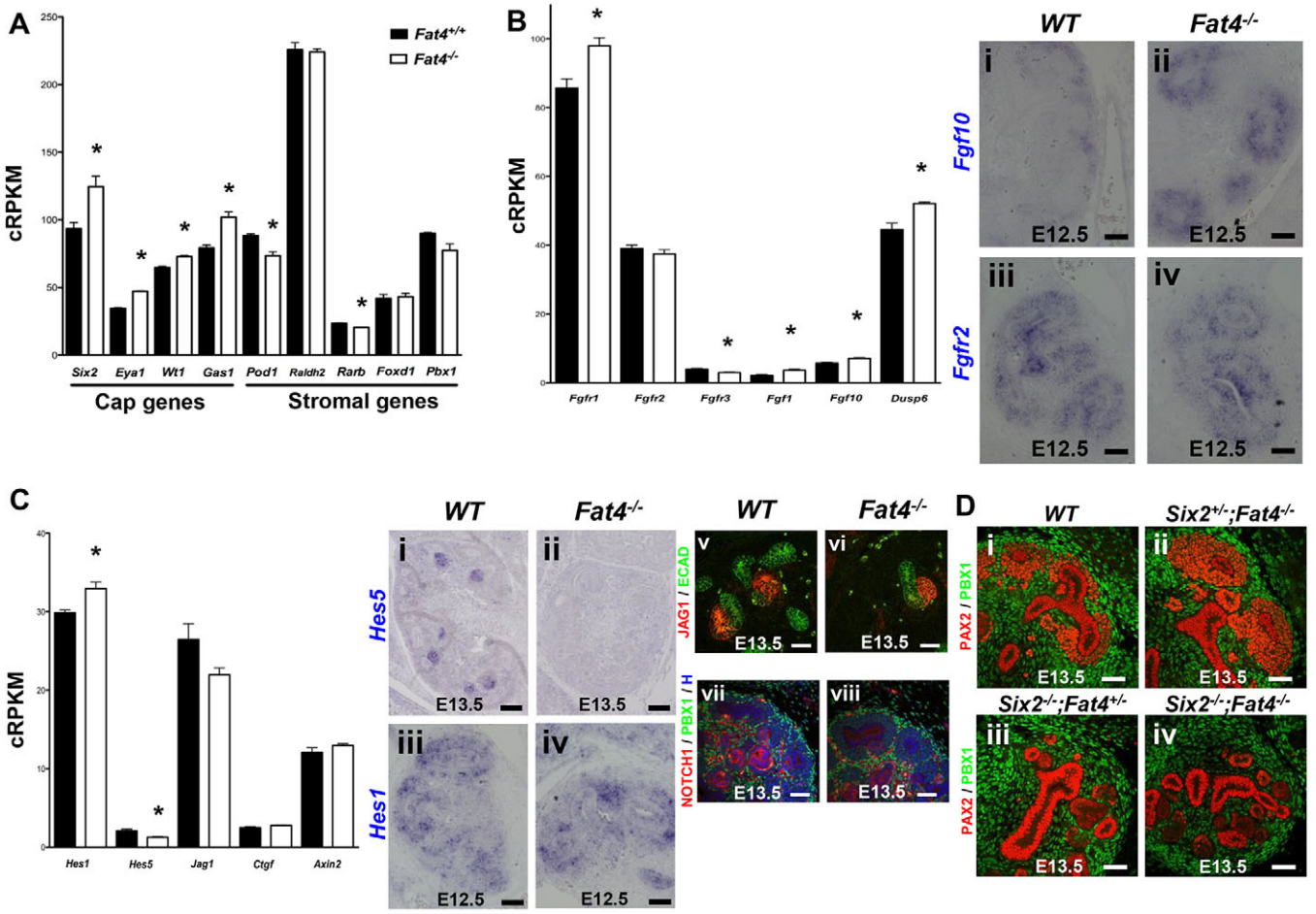

Fig. 7. Notch and FGF pathway components are misexpressed in *Fat4* mutants. (A-C) RNA sequencing of E13.5 $Fat4^{-/-}$ kidneys show that CM markers (*Six2*, *Eya1*, *Wt1* and *Gas1*) are increased compared with controls, whereas the stromal genes *Pod1* and *Rarb* are decreased in mutants (A). FGF signalling pathway components are misexpressed, including *Fgfr1*, *Fgf1* and *Fgf10* (B). ISH analysis of *Fgf10* confirms the increase in expression in $Fat4^{-/-}$ mutants (Bi, Bii), whereas *Fgfr2* expression is unaltered in mutants (Biii, Biv). Notch pathway genes are misexpressed (e.g. *Hes1/5*, *Jag1*), whereas the expression levels of *Axin2* (a β-catenin pathway gene) and *Ctgf* (downstream gene of *Yap*) do not change (C). Note that *Jag1* is reduced although this is not statistically significant (C). ISH and IF validation confirms that *Hes5* (Ci,Cii), JAG1 (Cv,Cvi) and NOTCH1 (Cvii,Cviii) expression are reduced, whereas *Hes1* (Ciii,Civ) does not alter in $Fat4^{-/-}$ mutants. cRPKM, corrected reads per kilobase of target transcript sequence per million of total reads. Differential expression of transcripts was computed between $Fat4^{+/+}$ control kidneys and $Fat4^{-/-}$ mutant kidneys for each gene. * $P<0.05$. (D) Loss of *Six2* results in precocious epithelialisation and a smaller CM population (Diii), whereas loss of *Fat4* results in reduced epithelialisation and a larger CM population (Dii) relative to control kidneys (Di). $Six2^{-/-};Fat4^{-/-}$ double mutants phenocopy $Six2^{-/-}$ single mutants (Div). All E13.5 kidneys were stained with PAX2 (CM and UB marker) and PBX1 (stromal marker). Scale bars: 100 µm in Ci, Cii; 50 µm in all other panels.

that TAZ could compensate for the loss of YAP. However, we see no increase in TAZ levels in *Fat4* mutants (data not shown), and loss of both YAP and TAZ in the CM does not cause an early block in CM renewal (Reginensi et al., 2013). Taken together, these data argue against a crucial role for either YAP or TAZ in the CM in *Fat4*-dependent nephron progenitor expansion. By contrast, we find that *Six2* is needed to maintain the progenitor pool (Kobayashi et al., 2008; Self et al., 2006). Our data indicate that *Six2* is needed for the expanded CM of $Fat4^{-/-}$ mutants, as $Six2^{-/-};Fat4^{-/-}$ mutants show loss of the characteristic expanded CM of *Fat4* mutants, and instead display the precocious epithelialisation of *Six2* mutants.

FAT4-DCHS1/2 signalling could be affecting progenitor maintenance, proliferation or the ability of the progenitors to commit and convert to an epithelial renal vesicle. *Wnt9b* induces the commitment of a subset of progenitors to an epithelial fate (Carroll et al., 2005). While canonical WNT signalling promotes epithelialisation, stabilisation of β-catenin blocks transition of induced CM to renal vesicles, and progression of the nephrogenic programme (Park et al., 2007). Thus, excess canonical signalling could also potentially account for the excess CM. However, we found no changes in the *TCF/Lef1-lacZ* WNT reporter in *Fat4* mutants (Saburi et al., 2008), nor in expression of the WNT target gene *Axin2*, suggesting that *Fat4* acts in a parallel pathway to *Wnt9b* to regulate progenitor gene expression and CM size. Terminal deoxynucleotidyl transferase dUTP nick end labelling (TUNEL) analysis shows a minor increase in cell death in *Fat4* mutants, and analysis of 5-ethynyl-2′-deoxyuridine (EdU) incorporation indicates that there is no increase in proliferation of the CM in *Fat4* mutants (supplementary material Fig. S5). Although decreased branching could lead to reduced division of CM at tips, we see no increase in the CM in *Vangl2* mutants, which also show reduced branching (Yates et al., 2010; M.B.-L., unpublished). Thus, we favour the hypothesis that loss of *Fat4* affects signalling from the stroma to *Dchs1/2* in the CM to alter progenitor self-renewal.

Development (2015) 142, 2564-2573 doi:10.1242/dev.122648

Our transcriptome analysis of *Fat4* mutants revealed previously unsuspected changes in genes involved in Notch and FGF-dependent signalling. Unravelling the contributions of these signalling pathways to Fat4-dependent regulation of progenitors will require double mutant/transgenic analyses of each of these pathways with *Fat4*. Genetic studies are also needed to understand the precise contribution of progenitor-regulating genes that have altered expression in *Fat4* mutants. Determining how *Fat4* and *Dchs1/2* control *Six2*-dependent progenitor differentiation/renewal will provide insights into how progenitor self-renewal is controlled, and may explain the renal hypoplasia observed in patients that harbour mutations in *FAT4* and *DCHS1* (Cappello et al., 2013; Mansour et al., 2012).

MATERIALS AND METHODS

Ethics statement

All mouse work was carried out in accordance with Ethics Canada, approved by the Animal Care Committee, and followed The Toronto Centre for Phenogenomics standard operating protocols.

Mouse strains

Fat4$^{-/-}$ and *Fat4*$^{flox/flox}$ (Saburi et al., 2008), *Fat4*$^{EGFP/EGFP}$ (Wu et al., 2008), *Dchs1*$^{-/-}$ (Mao et al., 2011), *Pax3*$^{Cre/+}$ (Engleka et al., 2005), *Pax2-Cre* (Ohyama and Groves, 2004), *Foxd1*$^{Cre/+}$ (Humphreys et al., 2010; Kobayashi et al., 2014), *Six2-Cre*^{TGC} (Kobayashi et al., 2008), *Hoxb7-Cre* (Zhao et al., 2004), *Rarb2-Cre* (Kobayashi et al., 2005), *Yap*$^{flox/flox}$ (Reginensi et al., 2013), *Rere*$^{-/-}$ (Zoltewicz et al., 2004), *Fat1*$^{-/-}$ (Ciani et al., 2003), *Fjx1*$^{-/-}$ (Probst et al., 2007) and *Vangl2*$^{Lp/+}$ (Strong and Hollander, 1949) mouse mutant alleles have all been previously described. The *Dchs2*$^{-/-}$ mouse mutant (international nomenclature *Dchs2*$^{tm1.2FHel}$) will be described fully elsewhere (F.H., unpublished). Briefly, a conditional allele (*Dchs2*$^{tm1.1FHel}$) was first generated by flanking the coding part of the last exon, encompassing the transmembrane and intracellular domains of *Dchs2*, with loxP sites. Mice carrying a constitutively deleted allele (*Dchs2*$^{tm1.2FHel}$) were produced by crossing the former with a germline-active deleter-cre mouse line [Tg(CMV-cre)1Cgn]. *Rere*$^{flox/flox}$ mice will be described fully elsewhere (H.P.Z., D.A.S., unpublished). Briefly, a recombineering strategy was used to generate a targeting vector in which the second coding exon of *Rere* was flanked by a 5′ loxP site and a 3′ FRT-flanked neo cassette and loxP site. *In vivo* excision of the neo cassette was achieved by crossing male mice carrying a correctly targeted *Rere* allele to female mice expressing the FLPe variant of the *Saccharomyces cerevisiae FLP1* recombinase gene in their germ line. On exposure to Cre, the second coding exon of the *Rere* flox allele is excised, resulting in a shift in the reading frame and generation of a premature stop codon. Presence of a vaginal plug on noon of the day when found was considered E0.5.

Histological analysis and electron microscopy

Standard Periodic acid-Schiff (PAS) staining was carried out according to (Reginensi et al., 2013).

EM was carried out on E12.5 kidneys fixed in 0.1 M cacodylate buffer (with 4% paraformaldehyde and 2% glutaraldehyde). Kidneys were fixed again in osmium tetroxide and embedded in Quetol-Spurr resin, and resin sections were stained with uranyl acetate and lead citrate and imaged under a FEI CM100 transmission electron microscope.

Nephron counting

Paraffin-embedded sections of newborn kidneys were cut at 7 µm thickness, stained with WT1 antibody and used to count the number of glomeruli per section, which was averaged for each kidney. A total of three wild-type and three mutant mice were compared.

In situ hybridisation

Digoxigenin-UTP labelled *Fat4*, *Fat1*, *Dchs1*, *Dchs2*, *Fgfr2*, *Fgf10*, *Hes1* and *Hes5* riboprobes were generated and samples processed according to Reginensi et al. (2013).

Immunofluorescence on paraffin sections and cryosections

IF was carried out on embryos embedded in paraffin according to standard protocols. Briefly, embryos were fixed overnight in 4% paraformaldehyde, washed in PBS, followed by serial dehydration with ethanol prior to embedding. Tissues were sectioned at 7 µm, deparaffinised, rehydrated, and boiled for 22 min with Antigen Unmasking Solution (H-3300, Vector Laboratories). Slides were blocked for an hour, probed overnight with primary antibodies and washed with PBS. FITC-, Alexa 488-, Cy3- or Cy5-conjugated secondary antibodies and Hoechst 33542 were added, and slides mounted with Vectashield. The following antibodies were used: SIX2 (ProteinTech; 11562-1-AP), pYAP (S127-Cell Signaling; 4911S), YAP (63.7; Santa Cruz; sc-101199), CITED1 (ThermoScientific; RB-9219-P0), PBX1b (Santa Cruz; sc-191852), WT1 (Dako; M3561), CDH1 (ECAD; BD Biosciences; 610181), CDH1 (ECAD) (rat; Invitrogen; 131900), PAX2 (Covance; PRB-276P), FOXD1 (generously provided by Dr Andy McMahon, University of Southern California, Los Angeles, USA), neural cell adhesion marker (NCAM; Sigma; C-9672), Sal-like 1 (SALL1; Abcam; AB31526), JAG1 (Cell Signaling; 2620), GFP (Abcam; ab13970) and IgG (Cell Signaling; 2729S). Frozen embryos were embedded in OCT and sectioned at 10 µm according to standard protocols. A tenascin C antibody from Sigma (T3413) was used. A Nikon D-Eclipse C1 confocal microscope was used to image all IF samples.

Quantification of SIX2$^+$ cells

Paraffin-embedded embryos cut at 7 µm were used to assess the number of SIX2$^+$ cells in embryonic kidneys. IF was carried out using SIX2 and ECAD antibodies to identify the CM and UB, respectively. SIX2$^+$ cells that surrounded a ureteric bud were quantified in ImageJ 1.43u (NIH, USA) using a macro that sets an autothreshold and runs the watershed option, thereby analysing particles that have clear outlines and were circular.

Immunoblotting

pYAP (5127-Cell Signaling) and GAPDH (Sigma) were used in immunoblots to assess pYAP protein levels in whole kidneys. Briefly, kidneys from E13.5 embryos were dissected, flash-frozen and stored at −80°C until further use. Tissues were homogenised in RIPA buffer using 23.5-G syringes, electrophoresed on 10% SDS-polyacrylamide gels and transferred onto PVDF membranes. Samples were blocked in 5% skimmed milk in TBS-Tween for 1 h at room temperature and incubated with primary and secondary antibodies. A Fluor-S MultiImager Max imager system was used to visualise samples following chemiluminescence detection.

TUNEL and EdU analyses

E12.5 embryos were processed for paraffin embedding and 7-µm sections were used for EdU incorporation assay and TUNEL analysis. For EdU analysis, 10 mg/ml of EdU was injected into pregnant dams 15 min prior to dissection of embryos. The Click-iT EdU Alexa Fluor 488 imaging kit from Life Technologies (C10337) was used to fluorescently label proliferating cells. TUNEL analysis was carried out according to Reginensi et al. (2013) using the Roche *In Situ* Cell Death Detection Kit (TMR red; 12 156 792 910).

RNA-sequencing

Gene expression analysis was performed using RNA-Seq data from three wild-type and three *Fat4* mutant samples by determining values for ‘corrected reads per kilobase per million reads’ (cRPKM), essentially as previously described (Labbé et al., 2012) and using the vast-tools pipeline (Irimia et al., 2014). Briefly, cRPKM values represent the number of unique-mapping reads per kilobase of transcript, after length-correction to account for multiple mapping positions. The corrected length is then used to divide the raw read counts per million mapped reads for each gene. The RNA-Seq datasets comprised 100 million paired-end, 101-mer reads. To assess significant fold differences between samples, an unpaired, uncorrected Student’s *t*-test was computed with a 0.05 *P*-value cutoff to determine differentially expressed transcripts. All data have been submitted to Gene Expression Omnibus under the accession number GSE70452.

Development (2015) 142, 2564-2573 doi:10.1242/dev.122648

Statistical analyses

All data are expressed as mean values with error bars representing standard error of the means (s.e.m.). An unpaired two-tailed Student's *t*-test was used to determine differences between two groups. To examine for significant differences among groups, data were subjected to a one-way analysis of variance (ANOVA). When statistical differences were found by one-way ANOVA, a Tukey's multiple comparison post-hoc test was conducted to delineate significance between groups. A fiducial limit of $P \leq 0.05$ was used throughout. All statistical analyses were conducted using GraphPad Prism 5.0a software.

Acknowledgements

We thank Ken Irvine (Rutgers University) for the *Dchs1*$^{-/-}$ mice; Jeff Wrana (Lunenfeld-Tanenbaum Research Institute) for the *Yap*$^{flox/flox}$ mice; Carl Bates (University of Pittsburgh) for the *Hoxb7-Cre* mice; Andy McMahon (University of Southern California) and Akio Kobayashi (University of Washington) for the *Six2-Cre*, *Six2*$^{+/-}$ and *Foxd1*$^{Cre/+}$ mice; and Mario Cappecchi for the *Fat4*$^{EGFP/+}$ mouse line (University of Utah). We are grateful to Doug Homyard for all electron microscopy analyses.

Competing interests

The authors declare no competing or financial interests.

Author contributions

M.B.-L. designed experiments and performed and analysed all results unless otherwise stated. A.R. carried out ISH and PAS experiments, and gathered embryos for EM analysis. Q.P. and B.J.B. carried out the RNA-seq analysis. H.P.Z. and D.A.S. created and provided the *Pax2-Cre; Rere*$^{flox/flox}$ embryos/mice. F.H. created and provided the *Dchs2*$^{-/-}$ embryos/mice. H.M. supervised, designed and interpreted all results. All authors edited the manuscript; M.B.-L. and H.M. wrote the manuscript.

Funding

This work was funded by an Ontario Graduate Scholarship (M.B.-L.); a Canadian Institutes of Health Research award [MOP 84468 to H.M.]; the March of Dimes [Cell Lineage and Differentiation Research grant no. 1-FY11-506 to H.M.]; and the Kidney Foundation of Canada [090014 to H.M.].

Supplementary material

Supplementary material available online at
http://dev.biologists.org/lookup/suppl/doi:10.1242/dev.122648/-/DC1

References

Babayeva, S., Zilber, Y. and Torban, E. (2011). Planar cell polarity pathway regulates actin rearrangement, cell shape, motility, and nephrin distribution in podocytes. *Am. J. Physiol. Renal. Physiol.* **300**, F549-F560.

Barlow, J. L., Drynan, L. F., Hewett, D. R., Holmes, L. R., Lorenzo-Abalde, S., Lane, A. L., Jolin, H. E., Pannell, R., Middleton, A. J., Wong, S. H. et al. (2010). A p53-dependent mechanism underlies macrocytic anemia in a mouse model of human 5q– syndrome. *Nat. Med.* **16**, 59-66.

Batourina, E., Gim, S., Bello, N., Shy, M., Clagett-Dame, M., Srinivas, S., Costantini, F. D. and Mendelsohn, C. L. (2001). Vitamin A controls epithelial/mesenchymal interactions through Ret expression. *Nat. Genet.* **27**, 74-78.

Bennett, F. C. and Harvey, K. F. (2006). Fat cadherin modulates organ size in Drosophila via the Salvador/Warts/Hippo signaling pathway. *Curr. Biol.* **16**, 2101-2110.

Boyle, S. C., Kim, M., Valerius, M. T., McMahon, A. P. and Kopan, R. (2011). Notch pathway activation can replace the requirement for Wnt4 and Wnt9b in mesenchymal-to-epithelial transition of nephron stem cells. *Development* **138**, 4245-4254.

Bryant, P. J., Huettner, B., Held, L. I., Jr, Reyerse, J. and Szidonya, J. (1988). Mutations at the fat locus interfere with cell proliferation control and epithelial morphogenesis in Drosophila. *Dev. Biol.* **129**, 541-554.

Cappello, S., Gray, M. J., Badouel, C., Lange, S., Einsiedler, M., Srour, M., Chitayat, D., Hamdan, F. F., Jenkins, Z. A., Morgan, T. et al. (2013). Mutations in genes encoding the cadherin receptor-ligand pair DCHS1 and FAT4 disrupt cerebral cortical development. *Nat. Genet.* **45**, 1300-1308.

Carroll, T. J., Park, J.-S., Hayashi, S., Majumdar, A. and McMahon, A. P. (2005). Wnt9b plays a central role in the regulation of mesenchymal to epithelial transitions underlying organogenesis of the mammalian urogenital system. *Dev. Cell* **9**, 283-292.

Chera, S., Ghila, L., Dobretz, K., Wenger, Y., Bauer, C., Buzgariu, W., Martinou, J.-C. and Galliot, B. (2009). Apoptotic cells provide an unexpected source of Wnt3 signaling to drive hydra head regeneration. *Dev. Cell* **17**, 279-289.

Ciani, L., Patel, A., Allen, N. D. and ffrench-Constant, C. (2003). Mice lacking the giant protocadherin mFAT1 exhibit renal slit junction abnormalities and a partially penetrant cyclopia and anophthalmia phenotype. *Mol. Cell. Biol.* **23**, 3575-3582.

Cullen-McEwen, L. A., Caruana, G. and Bertram, J. F. (2005). The where, what and why of the developing renal stroma. *Nephron. Exp. Nephrol.* **99**, e1-e8.

Das, A., Tanigawa, S., Karner, C. M., Xin, M., Lum, L., Chen, C., Olson, E. N., Perantoni, A. O. and Carroll, T. J. (2013). Stromal–epithelial crosstalk regulates kidney progenitor cell differentiation. *Nat. Cell Biol.* **15**, 1035-1044.

Di Giovanni, V., Alday, A., Chi, L., Mishina, Y. and Rosenblum, N. D. (2011). Alk3 controls nephron number and androgen production via lineage-specific effects in intermediate mesoderm. *Development* **138**, 2717-2727.

Di Giovanni, V., Walker, K. A., Bushnell, D., Schaefer, C., Sims-Lucas, S., Puri, P. and Bates, C. M. (2015). Fibroblast growth factor receptor–Frs2α signaling is critical for nephron progenitors. *Dev. Biol.* **400**, 82-93.

Engleka, K. A., Gitler, A. D., Zhang, M., Zhou, D. D., High, F. A. and Epstein, J. A. (2005). Insertion of Cre into the Pax3 locus creates a new allele of Splotch and identifies unexpected Pax3 derivatives. *Dev. Biol.* **280**, 396-406.

Fanto, M. and McNeill, H. (2004). Planar polarity from flies to vertebrates. *J. Cell Sci.* **117**, 527-533.

Fanto, M., Clayton, L., Meredith, J., Hardiman, K., Cahrroux, B., Kerridge, S. and McNeill, H. (2003). The tumor-suppressor and cell adhesion molecule Fat controls planar polarity via physical interactions with Atrophin, a transcriptional co-repressor. *Development* **130**, 763-774.

Hatini, V., Huh, S. O., Herzlinger, D., Soares, V. C. and Lai, E. (1996). Essential role of stromal mesenchyme in kidney morphogenesis revealed by targeted disruption of Winged Helix transcription factor BF-2. *Genes Dev.* **10**, 1467-1478.

Huang, Q., Li, F., Liu, X., Li, W., Shi, W., Liu, F.-F., O'Sullivan, B., He, Z., Peng, Y., Tan, A.-C. et al. (2011). Caspase 3–mediated stimulation of tumor cell repopulation during cancer radiotherapy. *Nat. Med.* **17**, 860-866.

Hum, S., Rymer, C., Schaefer, C., Bushnell, D. and Sims-Lucas, S. (2014). Ablation of the renal stroma defines its critical role in nephron progenitor and vasculature patterning. *PLoS ONE* **9**, e88400.

Humphreys, B. D., Lin, S.-L., Kobayashi, A., Hudson, T. E., Nowlin, B. T., Bonventre, J. V., Valerius, M. T., McMahon, A. P. and Duffield, J. S. (2010). Fate tracing reveals the pericyte and not epithelial origin of myofibroblasts in kidney fibrosis. *Am. J. Pathol.* **176**, 85-97.

Irimia, M., Weatheritt, R. J., Ellis, J. D., Parikshak, N. N., Gonatopoulos-Pournatzis, T., Babor, M., Quesnel-Vallieres, M., Tapial, J., Raj, B., O'Hanlon, D. et al. (2014). A highly conserved program of neuronal microexons is misregulated in autistic brains. *Cell* **159**, 1511-1523.

Kobayashi, A., Kwan, K.-M., Carroll, T. J., McMahon, A. P., Mendelsohn, C. L. and Behringer, R. R. (2005). Distinct and sequential tissue-specific activities of the LIM-class homeobox gene Lim1 for tubular morphogenesis during kidney development. *Development* **132**, 2809-2823.

Kobayashi, A., Valerius, M. T., Mugford, J. W., Carroll, T. J., Self, M., Oliver, G. and McMahon, A. P. (2008). Six2 defines and regulates a multipotent self-renewing nephron progenitor population throughout mammalian kidney development. *Cell Stem Cell* **3**, 169-181.

Kobayashi, A., Mugford, J. W., Krautzberger, A. M., Naiman, N., Liao, J. and McMahon, A. P. (2014). Identification of a multipotent self-renewing stromal progenitor population during mammalian kidney organogenesis. *Stem Cell Rep.* **3**, 650-662.

Labbé, R. M., Irimia, M., Currie, K. W., Lin, A., Zhu, S. J., Brown, D. D., Ross, E. J., Voisin, V., Bader, G. D., Blencowe, B. J. et al. (2012). A comparative transcriptomic analysis reveals conserved features of stem cell pluripotency in planarians and mammals. *Stem Cells* **30**, 1734-1745.

Levinson, R. S., Batourina, E., Choi, C., Vorontchikhina, M., Kitajewski, J. and Mendelsohn, C. L. (2005). Foxd1-dependent signals control cellularity in the renal capsule, a structure required for normal renal development. *Development* **132**, 529-539.

Li, W., Hartwig, S. and Rosenblum, N. D. (2014). Developmental origins and functions of stromal cells in the normal and diseased mammalian kidney. *Dev. Dyn.* **243**, 853-863.

Mansour, S., Swinkels, M., Terhal, P. A., Wilson, L. C., Rich, P., Van Maldergem, L., Zwijnenburg, P. J. G., Hall, C. M., Robertson, S. P. and Newbury-Ecob, R. (2012). Van Maldergem syndrome: further characterisation and evidence for neuronal migration abnormalities and autosomal recessive inheritance. *Eur. J. Hum. Genet.* **20**, 1024-1031.

Mao, Y., Mulvaney, J., Zakaria, S., Yu, T., Morgan, K. M., Allen, S., Basson, M. A., Francis-West, P. and Irvine, K. D. (2011). Characterization of a Dchs1 mutant mouse reveals requirements for Dchs1-Fat4 signaling during mammalian development. *Development* **138**, 947-957.

Mao, Y., Francis-West, P. and Irvine, K. D. (2015) A Fat4-Dchs1 signal between stromal and cap mesenchyme cells influences nephrogenesis and ureteric bud branching. *Development* **142**, 2574-2585.

Matakatsu, H. and Blair, S. S. (2006). Separating the adhesive and signaling functions of the Fat and Dachsous protocadherins. *Development* **133**, 2315-2324.

Mendelsohn, C. L., Lohnes, D., Decimo, D., Lufkin, T., LeMeur, M., Chambon, P. and Mark, M. (1994). Function of the retinoic acid receptors (RARs) during

development (II) Multiple abnormalities at various stages of organogenesis in RAR double mutants. *Development* **120**, 2749-2771.
Mendelsohn, C. L., Batourina, E., Fung, S., Gilbert, T. and Dodd, J. (1999). Stromal cells mediate retinoid-dependent functions essential for renal development. *Development* **126**, 1139-1148.
Ohyama, T. and Groves, A. K. (2004). Generation of Pax2-Cre mice by modification of a Pax2 bacterial artificial chromosome. *Genesis* **38**, 195-199.
Pan, G., Feng, Y., Ambegaonkar, A. A., Sun, G., Huff, M., Rauskolb, C. and Irvine, K. D. (2013). Signal transduction by the Fat cytoplasmic domain. *Development* **140**, 831-842.
Park, J.-S., Valerius, M. T. and McMahon, A. P. (2007). Wnt/beta-catenin signaling regulates nephron induction during mouse kidney development. *Development* **134**, 2533-2539.
Paroly, S. S., Wang, F., Spraggon, L., Merregaert, J., Batourina, E., Tycko, B., Schmidt-Ott, K. M., Grimmond, S., Little, M. and Mendelsohn, C. L. (2013). Stromal protein Ecm1 regulates ureteric bud patterning and branching. *PLoS ONE* **8**, e84155.
Probst, B., Rock, R., Gessler, M., Vortkamp, A. and Püschel, A. W. (2007). The rodent Four-jointed ortholog Fjx1 regulates dendrite extension. *Dev. Biol.* **312**, 461-470.
Quaggin, S. E., Schwartz, L., Cui, S., Igarashi, P., Deimling, J., Post, M. and Rossant, J. (1999). The basic-helix-loop-helix protein Pod1 is critically important for kidney and lung organogenesis. *Development* **126**, 5771-5783.
Rawls, A. S., Guinto, J. B. and Wolff, T. (2002). The cadherins fat and dachsous regulate dorsal/ventral signaling in the Drosophila eye. *Curr. Biol.* **12**, 1021-1026.
Reginensi, A., Scott, R. P., Gregorieff, A., Bagherie-Lachidan, M., Chung, C., Lim, D.-S., Pawson, T., Wrana, J. and McNeill, H. (2013). Yap- and Cdc42-dependent nephrogenesis and morphogenesis during mouse kidney development. *PLoS Genet.* **9**, e1003380.
Rock, R., Schrauth, S. and Gessler, M. (2005). Expression of mouse dchs1, fjx1, and fat-j suggests conservation of the planar cell polarity pathway identified in Drosophila. *Dev. Dyn.* **234**, 747-755.
Saburi, S., Hester, I., Fischer, E., Pontoglio, M., Eremina, V., Gessler, M., Quaggin, S. E., Harrison, R., Mount, R. and McNeill, H. (2008). Loss of Fat4 disrupts PCP signaling and oriented cell division and leads to cystic kidney disease. *Nat. Genet.* **40**, 1010-1015.
Saburi, S., Hester, I., Goodrich, L. and McNeill, H. (2012). Functional interactions between Fat family cadherins in tissue morphogenesis and planar polarity. *Development* **139**, 1806-1820.
Schnabel, C. A., Godin, R. E. and Cleary, M. L. (2003). Pbx1 regulates nephrogenesis and ureteric branching in the developing kidney. *Dev. Biol.* **254**, 262-276.
Self, M., Lagutin, O. V., Bowling, B., Hendrix, J., Cai, Y., Dressler, G. R. and Oliver, G. (2006). Six2 is required for suppression of nephrogenesis and progenitor renewal in the developing kidney. *EMBO J.* **25**, 5214-5228.
Sharma, P. and McNeill, H. (2013). Fat and Dachsous cadherins. *Prog. Mol. Biol. Transl. Sci.* **116**, 215-235.
Silva, E., Tsatskis, Y., Gardano, L., Tapon, N. and McNeill, H. (2006). The tumor-suppressor gene fat controls tissue growth upstream of expanded in the hippo signaling pathway. *Curr. Biol.* **16**, 2081-2089.
Simons, M. and Mlodzik, M. (2008). Planar cell polarity signaling: from fly development to human disease. *Annu. Rev. Genet.* **42**, 517-540.
Sing, A., Tsatskis, Y., Fabian, L., Hester, I., Rosenfeld, R., Serricchio, M., Yau, N., Bietenhader, M., Shanbhag, R., Jurisicova, A. et al. (2014). The atypical cadherin fat directly regulates mitochondrial function and metabolic state. *Cell* **158**, 1293-1308.
Smith-Bolton, R. K., Worley, M. I., Kanda, H. and Hariharan, I. K. (2009). Regenerative growth in Drosophila imaginal discs is regulated by Wingless and Myc. *Dev. Cell* **16**, 797-809.
Strong, L. C. and Hollander, W. F. (1949). Hereditary loop-tail in the house mouse: accompanied by imperforate vagina and craniorachischisis when homozygous. *J. Hered.* **40**, 329-334.
Willecke, M., Hamaratoglu, F., Kango-Singh, M., Udan, R., Chen, C.-l., Tao, C., Zhang, X. and Halder, G. (2006). The fat cadherin acts through the hippo tumor-suppressor pathway to regulate tissue size. *Curr. Biol.* **16**, 2090-2100.
Willecke, M., Hamaratoglu, F., Sansores-Garcia, L., Tao, C. and Halder, G. (2008). Boundaries of Dachsous Cadherin activity modulate the Hippo signaling pathway to induce cell proliferation. *Proc. Natl. Acad. Sci. USA* **105**, 14897-14902.
Wu, S., Ying, G., Wu, Q. and Capecchi, M. R. (2008). A protocol for constructing gene targeting vectors: generating knockout mice for the cadherin family and beyond. *Nat. Protoc.* **3**, 1056-1076.
Yang, C. H., Axelrod, J. D. and Simon, M. A. (2002). Regulation of Frizzled by fat-like cadherins during planar polarity signaling in the Drosophila compound eye. *Cell* **108**, 675-688.
Yates, L. L., Papakrivopoulou, J., Long, D. A., Goggolidou, P., Connolly, J. O., Woolf, A. S. and Dean, C. H. (2010). The planar cell polarity gene Vangl2 is required for mammalian kidney-branching morphogenesis and glomerular maturation. *Hum. Mol. Genet.* **19**, 4663-4676.
Zhao, H., Kegg, H., Grady, S., Truong, H.-T., Robinson, M. L., Baum, M. and Bates, C. M. (2004). Role of fibroblast growth factor receptors 1 and 2 in the ureteric bud. *Dev. Biol.* **276**, 403-415.
Zoltewicz, J. S., Stewart, N. J., Leung, R. and Peterson, A. S. (2004). Atrophin 2 recruits histone deacetylase and is required for the function of multiple signaling centers during mouse embryogenesis. *Development* **131**, 3-14.

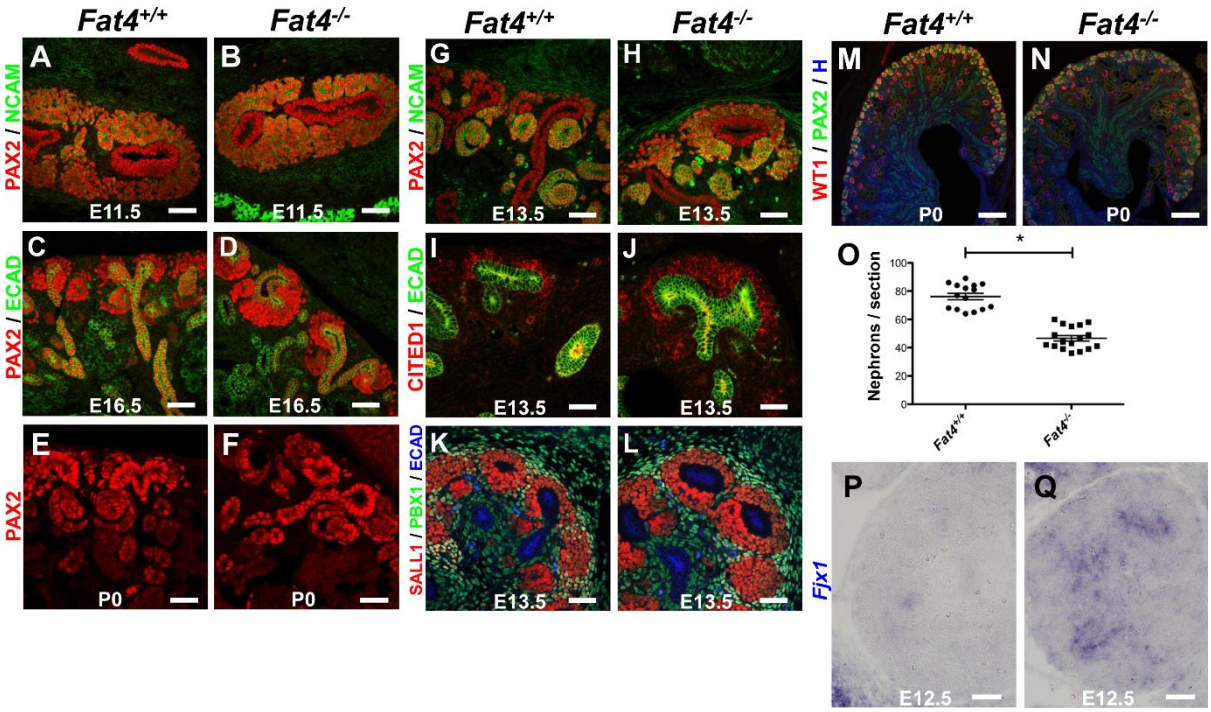

Suppl. Fig. S1: Early and late characterization of the expanded renal progenitor pool in *Fat4* mutants.

Fat4 mutants have a normal CM population early during kidney development E11.5 (A,B); however, the expansion of the CM persists until E16.5 and birth (P0) in *Fat4*$^{-/-}$ kidneys (C-F). Kidneys were stained for PAX2 and NCAM or ECAD using IF. PAX2, CITED1 and SALL1 also confirm that this expansion is due to renal progenitors (G-L). IF staining of *Fat4*$^{-/-}$ and wild-type control P0 kidneys with WT1 (glomeruli/nephron marker) and PAX2 (CM + UB marker) confirm reduced nephron numbers in mutants (M,N). Quantification of the number of glomeruli confirm that this is statistically significant ($p < 0.01$), denoted by * (O). The Hippo and planar cell polarity gene *Fjx1* is increased in E13.5 *Fat4* mutants (P,Q). H, Hoechst. All scale bars: 50 µm, except in M,N: 200 µm.

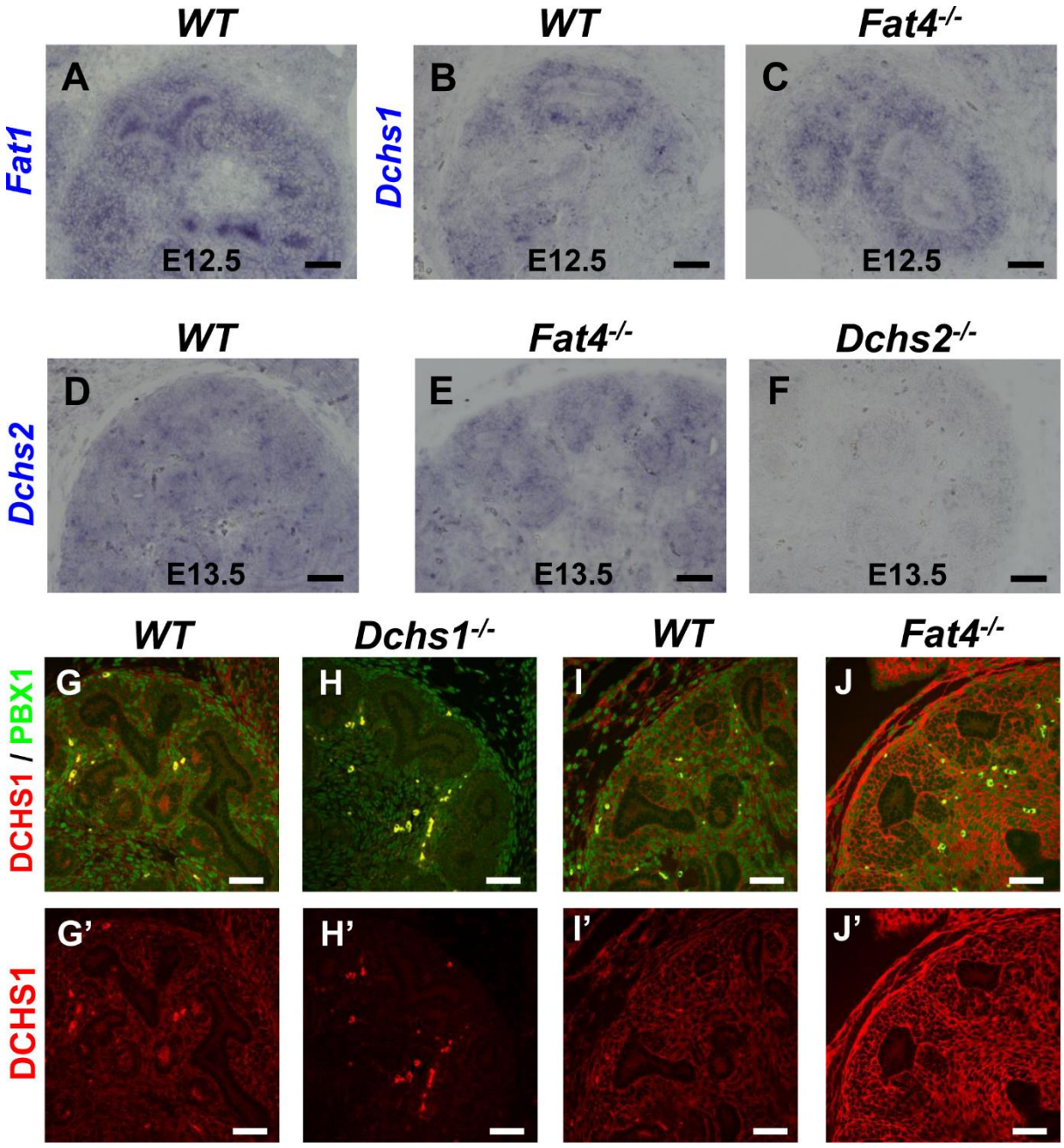

Suppl. Fig. S2: *Fat1*, *Dchs1* and *Dchs2* are expressed in the developing mouse kidney. ISH analysis shows that Fat1 is predominantly expressed in the UB, with moderate expression in the CM and weak expression in the stroma (A). *Dchs1* expression is increased in *Fat4*$^{-/-}$ mutants (C versus B), which is confirmed by IF analyses using a DCHS1 antibody (J versus I). The DCHS1 antibody is lost in *Dchs1*$^{-/-}$ mutants, confirming specificity of the antibody (G,H). *Dchs2* is expressed throughout the wildtype kidney (D) and is also present in *Fat4*$^{-/-}$ mutants (E). *Dchs2* expression is lost in *Dchs2*$^{-/-}$ mutants (F). Scale bars: 50 µm.

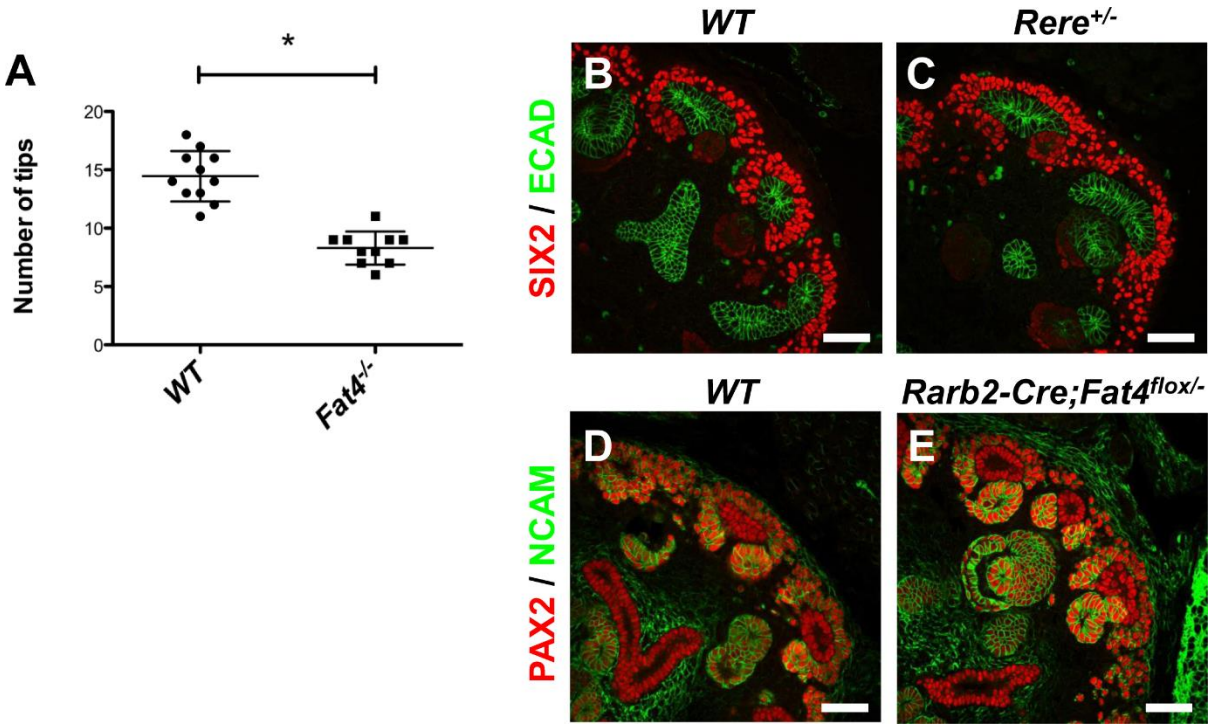

Suppl. Fig. S3: *Fat4* mutants have reduced branching, and removal of *Fat4* from the medullary stroma does not affect the renal progenitor pool.

E11.5 kidneys were grown for 48 h and UB tips were counted in both wild type and *Fat4*$^{-/-}$ mutants, which is quantified in A ($p < 0.0001$, denoted by *). *Fat4*$^{-/-}$ mutants show a significant decrease in branching when compared to wild-type kidneys. *Rere* heterozygotes have a normal CM similar to wildtype (B,C). Using *Rarb2-Cre*, *Fat4* was excised from the CM and medullary stromal populations, which did not disrupt the renal progenitor pool (D,E). This is in contrast to removal of *Fat4* from the cortical stroma (using *Foxd1*$^{Cre/+}$), which has an expanded CM population (see Fig. 5F). E13.5 kidneys were stained with PAX2 (CM and UB marker) and NCAM (epithelial, CM and stromal marker). Scale bars: 50 µm.

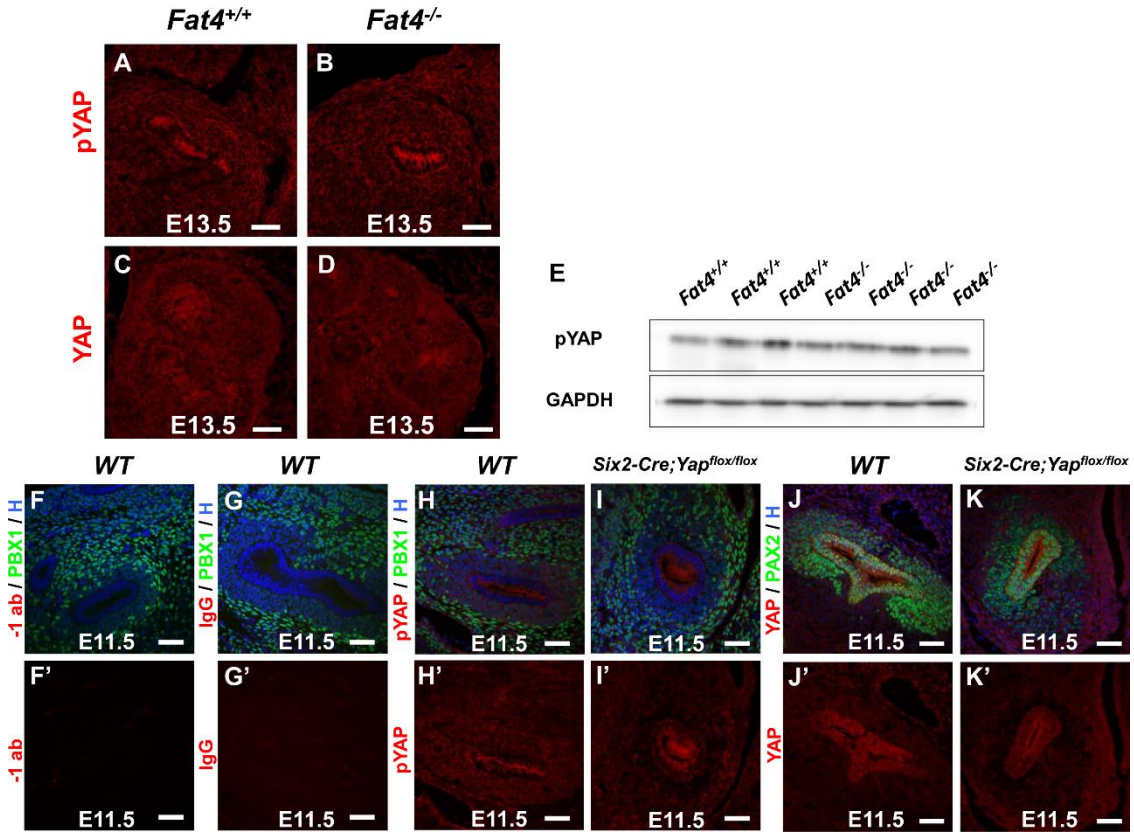

Suppl. Fig. S4: YAP expression is not altered in *Fat4* mutants.

IF analysis of E13.5 *Fat4* mutants reveals that they have normal phosphorylated-YAP (p-YAP; A,B) and YAP (C,D) expression levels and patterns. Western immunoblotting confirmed that pYAP expression is unchanged between E13.5 *Fat4* mutants and littermate controls (E). F and G show IF of E11.5 kidneys stained with no primary antibody and an IgG control, respectively, where no red signal is observed. Both pYAP and YAP are efficiently excised by *Six2-Cre* from the CM by E11.5 (compare I versus H, and K versus J). Scale bars: 50 µm.

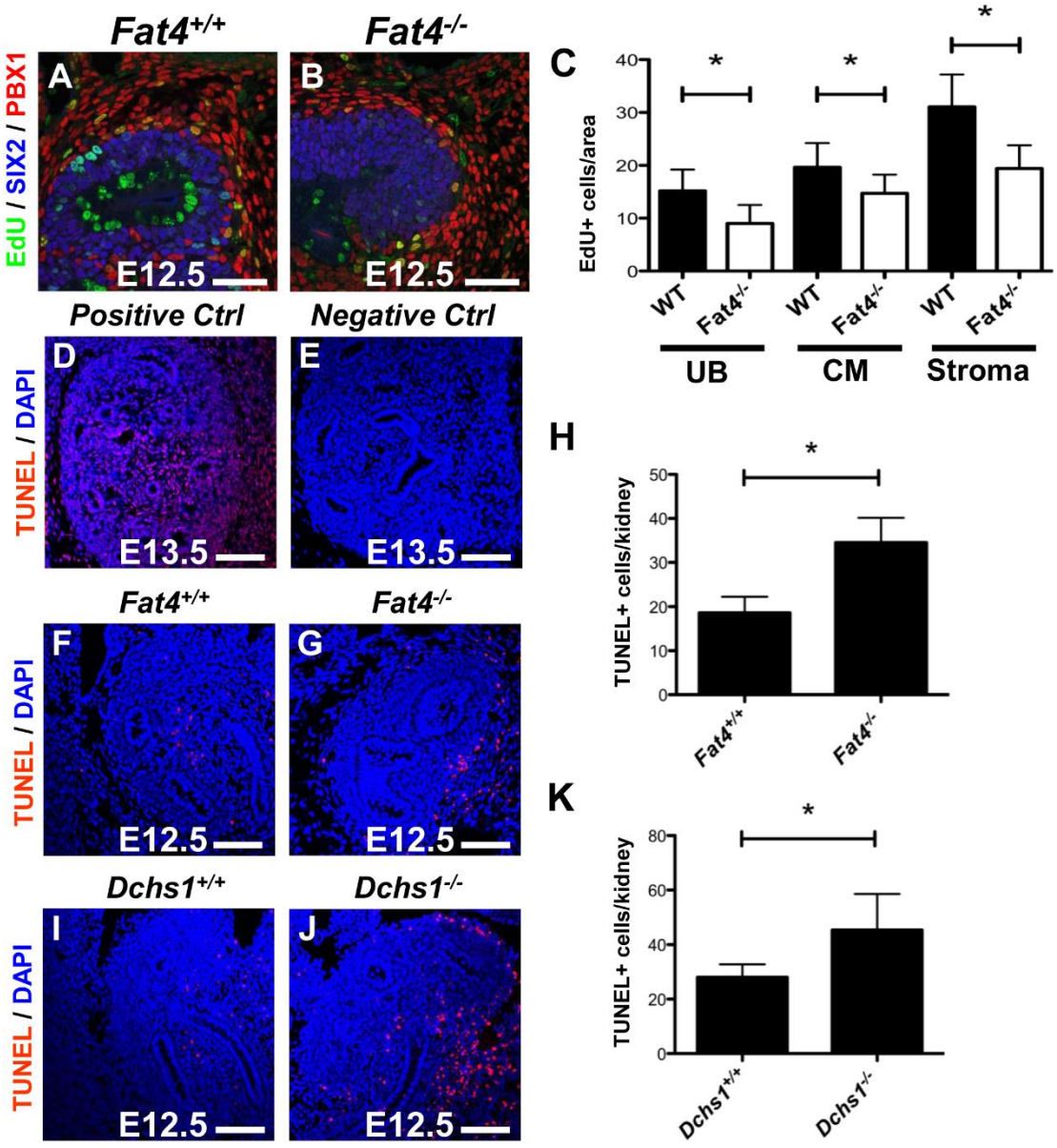

Suppl. Fig. S5: *Fat4* mutants do not show increased proliferation, and loss of *Dchs1* or *Fat4* results in increased apoptosis.

E12.5 *Fat4* mutant kidneys incorporated less EdU compared with wildtype controls (B versus A). EdU was quantified in each compartment (i.e. UB, CM or stroma) separately, where *Fat4* mutants had decreased EdU incorporation in each cell compartment as compared to controls (C; $p < 0.05$, denoted by *). TUNEL analysis revealed an increase in apoptosis in both *Fat4*$^{-/-}$ single mutants (F,G) and *Dchs1*$^{-/-}$ single mutants (I,J) at E12.5. H and K are quantifications of TUNEL-positive cells per kidney ($p < 0.05$, denoted by *). D is a DNAse I treated control slide, while E did not undergo terminal transferase treatment. Scale bars: A,B: 50 µm; D-G,I,J: 100 µm.